Current Biology 18, 1713–1717, November 11, 2008 ©2008 Elsevier Ltd All rights reserved DOI 10.1016/j.cub.2008.09.046

Report

Microtubule-Driven Multimerization Recruits ase1p onto Overlapping Microtubules

Lukas C. Kapitein,[1,2,4] Marcel E. Janson,[1,4,5] Siet M.J.L. van den Wildenberg,[1] Casper C. Hoogenraad,[2] Christoph F. Schmidt,[3] and Erwin J.G. Peterman[1,*]

[1]Department of Physics and Astronomy and Laser Centre
VU University Amsterdam
De Boelelaan 1081
1081 HV Amsterdam
The Netherlands

[2]Department of Neuroscience
Erasmus MC
Dr. Molewaterplein 50
3015 GE Rotterdam
The Netherlands

[3]Physikalisches Institut
Fakultät für Physik
Georg-August-Universität
Friedrich-Hund-Platz 1
37077 Göttingen
Germany

Summary

Microtubule (MT) crosslinking proteins of the ase1p/PRC1/Map65 family play a major role in the construction of MT networks such as the mitotic spindle. Most homologs in this family have been shown to localize with a remarkable specificity to sets of MTs that overlap with an antiparallel relative orientation [1–4]. Regulatory proteins bind to ase1p/PRC1/Map65 and appear to use the localization to set up precise spatial signals [5–10]. Here, we present evidence for a mechanism of localized protein multimerization underlying the specific targeting of ase1p, the fision yeast homolog. In controlled in vitro experiments, dimers of ase1-GFP diffused along the surface of single MTs and, at concentrations above a certain threshold, assembled into static multimeric structures. We observed that this threshold was significantly lower on overlapping MTs. We also observed diffusion and multimerization of ase1-GFP on MTs inside living cells, suggesting that a multimerization-driven localization mechanism is relevant in vivo. The domains responsible for MT binding and multimerization were identified via a series of ase1p truncations. Our findings show that cells use a finely tuned cooperative localization mechanism that exploits differences in the geometry and concentration of ase1p binding sites along single and overlapping MTs.

Results and Discussion

Velocity sedimentation and size-exclusion chromatography suggest that *S. cerevisiae* Ase1 forms an extended rod-shaped homodimer [3]. To examine the oligomeric state of *S. pombe* ase1p, we imaged single ase1-GFP complexes absorbed to a coverslip surface. Intensity time traces of individual fluorescent spots often revealed two bleaching steps (Figure 1C, inset), suggesting that complexes contained two ase1-GFP molecules. To confirm this result, we compared ase1-GFP prebleach intensity to that of dimeric Kinesin1-GFP and tetrameric Eg5-GFP [11] and found the intensity distribution of ase1-GFP (mean intensity ± SEM = 4.8 ± 0.2 × 10^3 a.u.) to overlap the distribution of the reference dimer (mean intensity ± SEM = 5.0 ± 0.2 × 10^3 a.u.), while being clearly distinct from that of tetrameric Eg5 (mean intensity ± SEM = 8.4 ± 0.3 × 10^3 a.u.; Figure 1C). Our data thus indicate that ase1-GFP was predominantly dimeric in the absence of MTs.

We next used a single-molecule assay to explore the dynamics and multimerization state of ase1-GFP while interacting with individual MTs. Biotin-labeled MTs were attached to a streptavidin-coated coverslip, and the surface was subsequently covered with a polymer brush to prevent further protein binding [12]. Finally, ase1-GFP molecules were added to the sample chamber at a low concentration (0.45 nM) and allowed to interact with the MTs (Figure 1A). We could observe ase1-GFP binding from solution to the MTs. Once attached, fluorescent proteins moved stochastically along the length of MTs (Figure 1B; Movie S1 available online). The average intensity of these moving spots was similar to the average intensity of surface-adsorbed ase1-GFP assayed under identical illumination conditions, indicating that these spots are primarily individual ase1-GFP dimers (Figures 1D and 1E).

To quantify the stochastic motion of the dimers, we tracked individual ase1-GFP dimers moving on MTs by using a subpixel-resolution tracking algorithm (Figure 1F). The mean square displacement (MSD) obtained from these traces increased linearly with time (Figure 1G) and could be fitted with a one-dimensional diffusion constant of 5.5 ± 0.5 × 10^4 nm^2 s^{-1} (see [11] and [13] for methods). The average length of time over which individual fluorescence spots could be observed on a MT was 11 ± 2 s (Figure 1H). This is a lower limit of the interaction time of dimers with MTs because photobleaching occurred on a similar time scale.

We then repeated the MT-binding experiment at a higher ase1-GFP concentration (4.5 nM) and found that very bright spots, which were not observed in the absence of MTs (data not shown), covered the MTs (Figure 2A; Movie S2). As opposed to the individual dimers observed at low concentration (Figure 1B), the bright spots did not diffuse measurably, but were statically bound to MTs for more than 10 min (Figure 2D). The average intensity of these spots was ~18 times that of a dimer (Figure 2B), suggesting that ase1-GFP dimers interact and form stable clusters. Formation of multimeric particles at high ase1-GFP concentrations was confirmed by spatial image correlation spectroscopy (see Supplemental Results and Discussion) [14]. The lower mobility of these multimers suggests that the additional protein-protein interactions involved are acting to reinforce ase1p-binding to MTs, leading to an increase of overall MT association. Indeed, the appearance of multimers between 0.45 and 4.5 nM goes hand in hand with a nonlinear increase of MT-bound ase1p (Figure 2C). This demonstrates that

*Correspondence: erwinp@nat.vu.nl
[4]These authors contributed equally to this work
[5]Present address: Laboratory of Plant Cell Biology, Wageningen University, Arboretumlaan 4, 6703 BD Wageningen, The Netherlands

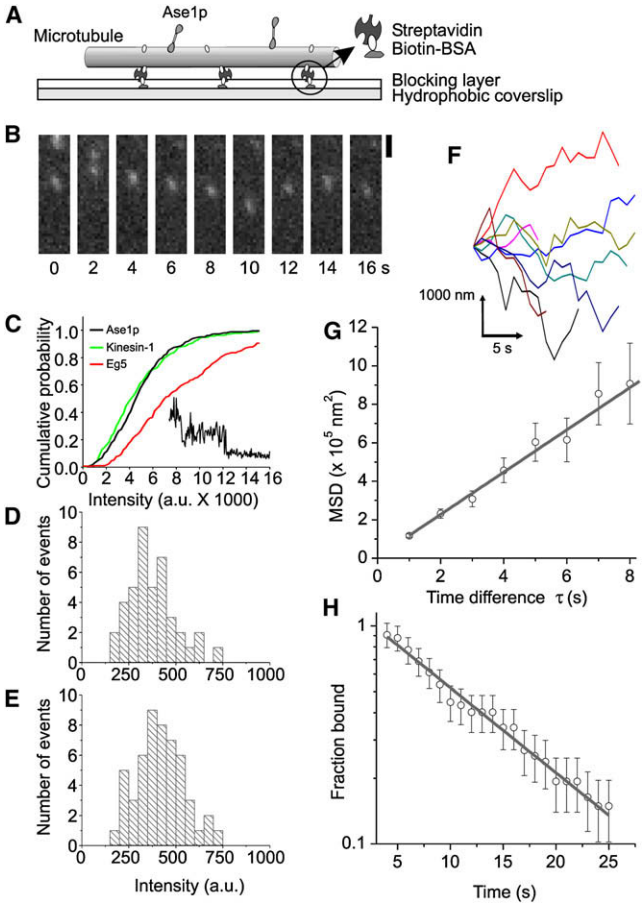

Figure 1. Ase1-GFP Dimers Diffuse along Single MTs

(A) Stabilized and biotinylated microtubules are immobilized on a hydrophobic surface that is coated with biotinylated BSA and further blocked with Pluronic. Streptavidin is used as a linker.

(B) Frames from a time-lapse recording showing diffusion of ase1-GFP (0.45 nM) along a line that corresponds with the position of an immobilized MT. Scale bar represents 2 μm.

(C) Cumulative histogram of initial fluorescence intensities of isolated surface-immobilized spots of ase1-GFP (n = 271), dimeric Kinesin-GFP (n = 198), and tetrameric Eg5-GFP (n = 264). Insert shows step-wise bleaching of isolated spots of ase1-GFP.

(D) Distribution of initial fluorescence intensities of isolated spots of ase1-GFP adsorbed to glass. The average intensity is 351 ± 19 (SEM, n = 41).

(E) Distribution of the initial fluorescence intensities of isolated spots of ase1-GFP bound to MTs as in (A). The average intensity is 410 ± 18 (SEM, n = 52).

(F) Eight representative tracks of moving ase1-GFP spots along MTs.

(G) Mean squared displacement (MSD) calculated from 54 ase1-GFP tracks. The solid line is a fit to a straight line: $MSD = 2D\tau$ + offset, with diffusion constant, $D = 5.5 \pm 0.5 \times 10^4$ nm^2 s^{-1}. Mean squared displacement (MSD ± SEM) calculated from 54 ase1p-GFP tracks.

(H) Plot of the fraction of mobile ase1-GFP spots that was still visibly attached to a MT after observation time t. The average binding time, t_{avg} = 11 ± 2 s, is obtained from the time constant of a single exponential fit (solid line). Plot of the fraction of mobile ase1p-GFP spots that were still visibly attached to a MT (±SEM) after observation time t.

ase1p dimers bind cooperatively to MTs, most likely as a result of multimer formation.

We next tried to directly visualize the cluster formation process, i.e., the addition of ase1-GFP dimers to existing multimers. After partial photobleaching of MT-bound multimers, the landing of new dimers could be observed even when occurring next to the initially much brighter multimers. At a high concentration of ase1-GFP (4.5 nM), dimers often appeared to bind directly from solution to a multimer (Figure 2D). In those cases we observed them to remain attached for on average 50 s (most likely limited by photobleaching), about 5 times longer than individual dimers on bare MTs (Figure 1H). The decrease in off-rate upon multimerization, and perhaps changes in on-rate, explain the nonlinear increase in MT-bound ase1-GFP (Figure 2C). At an intermediate concentration (1.5 nM), less multimers formed on the MTs, and we observed individual dimers to bind to bare sections of the MTs (Figure 2E). Subsequently, these dimers diffused along the MT surface and were in some cases observed to incorporate into a multimer after an encounter. These events increased the fluorescence intensity of the multimers (Figure 2F). The reverse process of a dimer releasing from a multimer and then diffusing along the MT was also observed (Figure 2F). These results demonstrate that the MT-driven multimerization of ase1p dimers is a dynamic process with continuous addition and removal of subunits.

With the localization of ase1p to overlapping MTs in mind, we next set out to study ase1p multimerization on pairs of MTs. We generated bundled MTs by mixing ase1p with polarity-marked MTs. Pairs of MTs were first scored for polarity after immobilization on a MT-binding coverslip to check for an orientational bias in the crosslinking mechanism. The majority of pairs were antiparallel (72% ± 4% for the 85 pairs for which the polarity could be determined unambiguously [mean ± standard deviation]). This was slightly more than found before at a lower ionic strength [1]. To determine the dynamics of ase1p binding to overlapping MTs, we did not use this simple assay because ase1p could get immobilized on the sticky surface. We used instead our single MT assay with blocked surfaces as described above (Figures 1 and 2), but supplemented the assay mix with a small number of nonbiotinylated MTs (Figure 3A). Pairs of MTs were found on the surface, indicating that the additional MTs had become linked to surface-bound MTs by ase1-GFP. At lower ase1-GFP concentrations (1.5 nM), few multimers were visible on single MTs, in agreement with Figure 2E. On crosslinked MT pairs, in contrast, many more multimers were observed (Figures 3B–3D). The presence of a second MT thus appeared to have the same effect as a higher ase1p concentration, or, in other words, the presence of a second MT lowered the multimerization threshold. This mechanism effectively targets ase1p to MT overlap zones. The specificity for overlap zones decreased at high ase1-GFP concentrations (4.5 nM) at which ase1-GFP multimers were observed both on individual MTs and on crosslinked pairs.

At low ase1-GFP concentrations (0.45 nM), individual dimers could be observed on both single and overlapping MTs, which allowed us to look for subtle differences in the ase1p-MT interaction that could trigger multimerization. We found that individual dimers between overlapping MTs diffused at a 15-fold slower rate (Figure S3), and we estimated that their interaction time was at least two times longer than the 11 s measured along single MTs (exact determination was not possible because of photobleaching) (Figure S3). This stronger interaction would lead to an increase of the local dimer concentration between MTs and might thereby locally elevate the system over the critical concentration threshold required for stable cluster formation. Additionally, dimers might become kinetically trapped in regions of low diffusivity [15]. We estimate, however, that the latter effect should contribute only negligibly to localization (Supplemental Results and Discussion). In

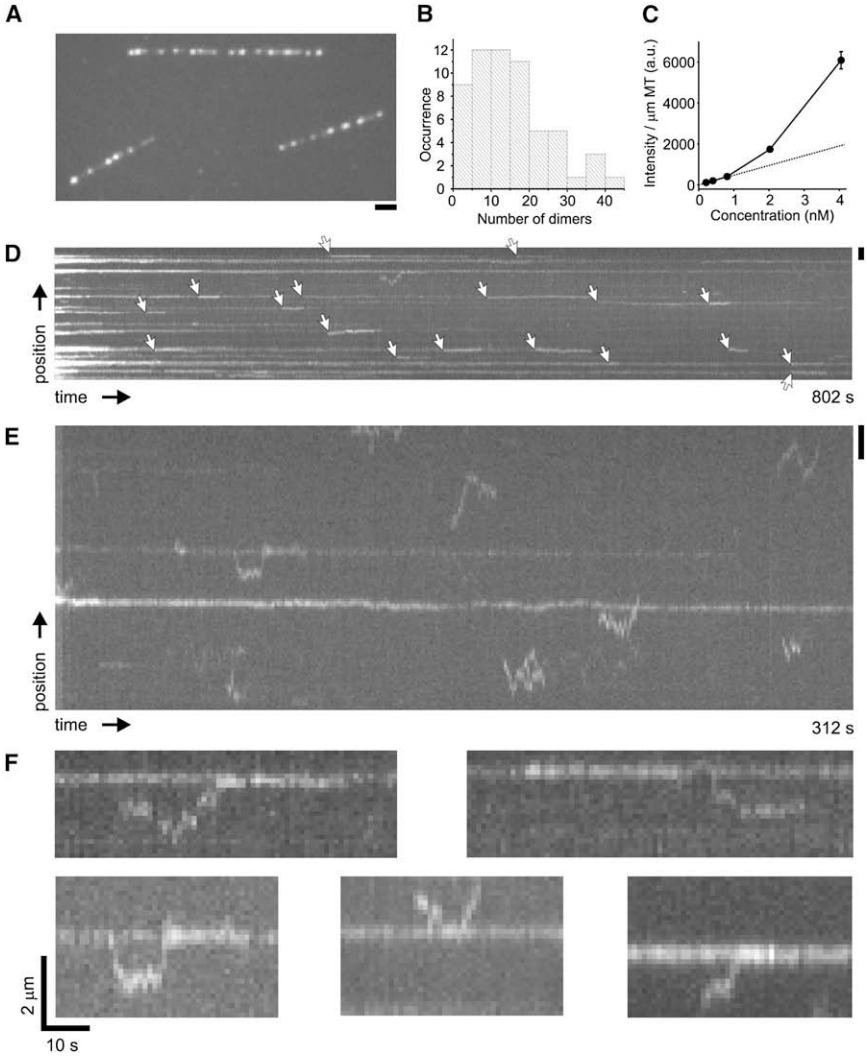

Figure 2. Ase1-GFP Multimerization on the MT Lattice

(A) Still frame showing the effect of an increased ase1-GFP concentration (4.5 nM). Ase1-GFP decorates MTs as bright and immobile multimers.

(B) Intensity distribution of ase1-GFP multimers, normalized by the measured intensity of single ase1-GFP dimers. The average intensity corresponds to 18 ± 4 ase1-GFP dimers (SEM, n = 50).

(C) Average fluorescence intensity (±SEM) of bound ase1-GFP per unit MT length as a function of ase1-GFP concentration. The first part of the curve appears linear (as indicated by the linear fit through the first three data points), but at higher ase1p concentrations, the fluorescence intensity increases nonlinearly, indicating cooperative binding. Error bars smaller than the symbol size are not drawn.

(D) Kymograph of a MT incubated with ase1-GFP at a high concentration (4.5 nM). Events of ase1-GFP dimers binding to a multimer directly out of solution are marked with an arrow.

(E) Kymograph of ase1-GFP along a MT at an intermediate concentration (1.5 nM). After initial binding, individual dimers exhibit lattice diffusion in between multimers. Multimers are photobleached because of prolonged exposure.

(F) Examples of dimers that bound to a multimer after lattice diffusion or released from a multimer (top right and bottom center).

Scale bars represent 2 µm.

conclusion, specific localization of ase1p appears to be a two-step process. Initially, ase1p dimers localize with higher affinity to overlapping MTs. Once a concentration threshold is crossed, dimers become further stabilized through interactions with neighboring ase1p dimers, lowering their off-rate substantially. These effects together can explain the remarkable preference of ase1p for overlapping MTs in cells.

Next, we investigated whether this mechanism of ase1p localization driven by multimerization is indeed relevant in cells. To this end, we imaged simultaneously mCherry-tubulin and ase1-GFP expressed in COS7 cells via fast, dual-color TIRF microscopy (see Supplemental Experimental Procedures). We chose COS7 cells because their large and flat lamellae provide a convenient geometry for observing ase1p-MT interactions. We observed MT bundling by ase1-GFP and localization of ase1-GFP predominantly on bundled MTs in high-intensity clusters with moderate mobility (Figures 4A and 4C; Movie

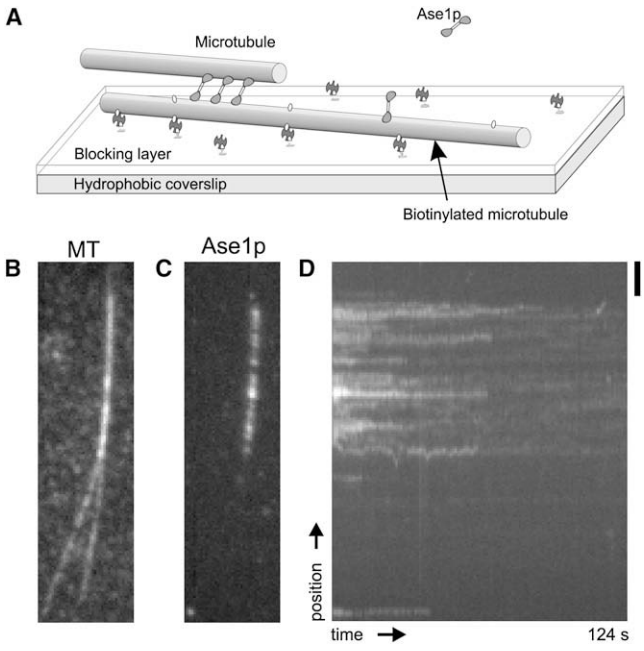

Figure 3. Specific ase1-GFP Multimerization between Two MTs

(A) Free-floating, nonbiotinylated MTs are added to the experiment described in Figure 1A. Subsequently, these become bundled by ase1-GFP to biotinylated MTs immobilized at the surface. Individual and overlapping MTs can be studied next to each other.

(B) Video frame showing two partially overlapping rhodamine-labeled MTs at intermediate ase1-GFP concentration (1.5 nM).

(C) Video frame of the ase1-GFP distribution along the MTs in (B). Ase1-GFP accumulates as numerous bright multimers at the section of overlap. Individual MTs are almost empty.

(D) Kymograph showing the dynamics of ase1-GFP multimers between the overlapping MTs in (B).

Scale bar represent 2 µm.

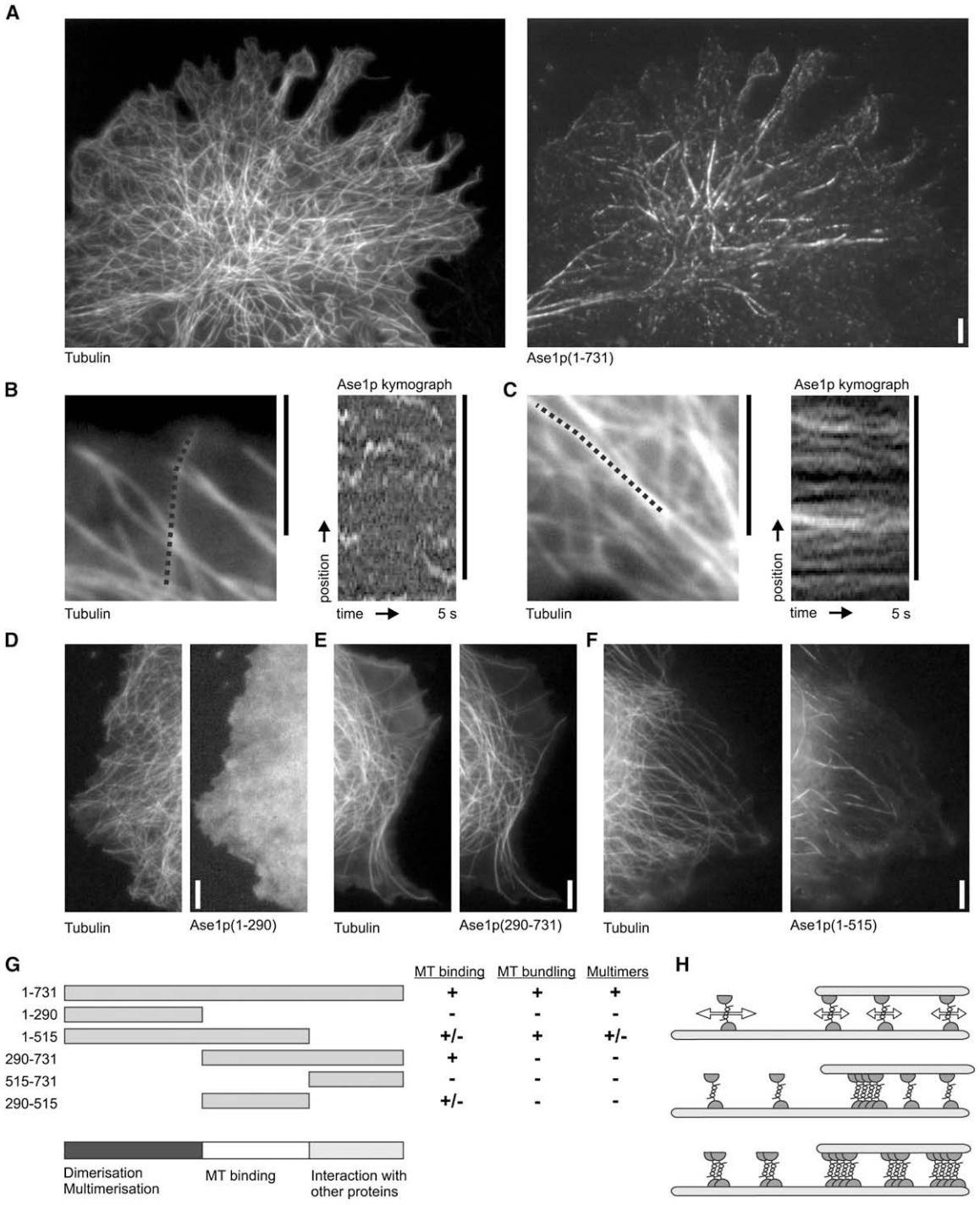

Figure 4. Ase1-GFP Dynamics and Domain Analysis in COS7 Cells

(A) COS7 cell simultaneously expressing Cherry-tubulin (left) and full-length ase1-GFP (right). Bright localization of ase1-GFP coincides with induced regions of MT overlap.

(B) Enlargement of a cell region with nonbundled MTs (left, average of 20 frames) with corresponding ase1-GFP dynamics show in a kymograph (right).

(C) Enlargement of bundled MTs (left, average of 20 frames) with corresponding ase1-GFP dynamics shown in a kymograph (right). Ase1-GFP localizes as less mobile spots that bind for a prolonged time. Prior to kymography, movies were filtered by convolution with the kernel described in [16].

(D) The N terminus of ase1p (aa 1–290 tagged with GFP) does not bind to MTs in COS7 cells. Bundling of MTs is not induced.

(E) A construct without N terminus (aa 290–731, tagged with GFP) binds homogenously along MTs. Bundling of MTs is not induced.

(F) A construct lacking the C terminus (aa 1–515, tagged with GFP) accumulates at overlapping MTs similar to the full-length protein.

(G) Summary of truncation experiments in COS7 cells. Multimer formation is assayed with kymography of overlapping MTs.

(H) Cartoon illustrating ase1 behavior in different geometries at different concentrations. Top: ase1 dimers diffuse faster and detach more rapidly on a single MT than between two crosslinked MTs. Middle and bottom: ase1 dimers form multimers on microtubules. At high ase1 concentrations (bottom), this happens both on single and bundled MTs; at lower concentrations (middle), multimerization occurs only between MT bundles.

Scale bars represent 5 μm.

S3). In addition, we observed dim mobile fluorescent spots, primarily on individual, nonoverlapping, MTs (Figures 4A and 4B; Movie S4). These results demonstrate that also inside cells, ase1-GFP both diffuses along MTs and gets enriched in regions of MT overlap in the form of multimers.

In order to identify which ase1p domains are involved in MT binding and multimerization, we expressed a series of truncated ase1-GFP constructs in COS7 cells (Figures 4D–4G). A C-terminal deletion construct (amino acid [aa] 1–515), previously shown to form dimers [1], localized to MT overlap zones like the full-length protein (Figure 4F). In contrast, a monomeric N-terminal deletion construct (aa 290–731) [1] binds MTs but does not bundle MTs nor assemble into multimeric structures (Figure 4E). Both the N-terminus (aa 1–290) and the C terminus (515–731) did not bind MTs, whereas the central domain (aa 290–515) binds MTs weakly. From this we conclude that the C terminus is not involved in dimerization and higher order multimerization, but instead, its main function might be to regulate interactions with various proteins such as cls1/peg1 (CLASP), as reported [6]. Ase1p's central region (most likely extending slightly beyond aa 515) mediates the diffusive interaction with the MT.

In summary, our in vitro experiments have demonstrated that the presence of a second aligned MT can switch a population of diffusively mobile ase1p dimers to stably bound ase1p multimers. The molecular mechanism likely involves subtle changes in the geometry, affinity, and concentration of ase1p binding sites between single and overlapping MTs. These small changes can be sufficient to trigger multimerization and subsequent large changes in protein localization. This highly nonlinear, switch-like phenomenon was also seen in vivo, in COS7 cells, and it explains why ase1p is found in cells with a striking abundance on overlapping MTs. The ability of ase1p to form a stable scaffold between the MTs of the spindle midzone makes it a crucial binding partner for several proteins that fulfill key roles in spindle organization and cytokinesis. Localization and targeting is typically thought of as a specific interaction between two proteins or a protein and a somehow chemically modified target. Alternatively, in our model, the physical arrangement and geometry of cellular structures, here overlapping MTs, provides the initial trigger for localization. Such a subtle physical scheme that exploits small differences in mobility and affinity together with nonlinear threshold behavior might be quite general and might, in addition to reaction-diffusion patterns, be the cell's ingenious way to achieve strong localization signals.

Supplemental Data

Supplemental Data include Supplemental Results and Discussion, Supplemental Experimental Procedures, five figures, and four movies and can be found with this article online at http://www.current-biology.com/supplemental/S0960-9822(08)01276-1.

Acknowledgments

We thank Zdenek Lansky for purification of ase1-GFP, Phebe Wulf en Nanda Keijzer (Erasmus MC) for cloning the β-actin-ase1 constructs, Sandra Ruf (EMBL, Heidelberg) for preparing Cy5-tubulin, Tarun Kapoor (Rockefeller University, NY) for the gift of Eg5-GFP, and Joost van Mameren for writing the kymography and tracking software. L.C.K. and E.J.G.P. were supported by a VIDI fellowship to E.J.G.P. from the Dutch Research Council for Earth and Life Sciences (ALW). L.C.K. was also supported by the Erasmus MC fellowship program. M.E.J. was supported by a VENI fellowship from ALW. C.C.H. was supported by European Science Foundation (European Young Investigators [EURYI] Award) and Human Frontier Science Program (HFSP-CDA). C.F.S. was supported by the Foundation for Fundamental Research on Matter (FOM), a Research Grant from the Human Frontier Science Program, and the DFG Center for Molecular Physiology of the Brain (CMPB).

Received: December 2, 2007
Revised: September 15, 2008
Accepted: September 15, 2008
Published online: October 30, 2008

References

1. Janson, M.E., Loughlin, R., Loïodice, I., Fu, C., Brunner, D., Nédélec, F.J., and Tran, P.T. (2007). Cross-linkers and motors organize dynamic microtubules to form stable bipolar arrays in fission yeast. Cell *128*, 357–368.
2. Loiodice, I., Staub, J., Setty, T.G., Nguyen, N.P.T., Paoletti, A., and Tran, P.T. (2005). Ase1p organizes antiparallel microtubule arrays during interphase and mitosis in fission yeast. Mol. Biol. Cell *16*, 1756–1768.
3. Schuyler, S.C., Liu, J.Y., and Pellman, D. (2003). The molecular function of Ase1p: Evidence for a MAP-dependent midzone-specific spindle matrix. J. Cell Biol. *160*, 517–528.
4. Yamashita, A., Sato, M., Fujita, A., Yamamoto, M., and Toda, T. (2005). The roles of fission yeast Ase1 in mitotic cell division, meiotic nuclear oscillation, and cytokinesis checkpoint signaling. Mol. Biol. Cell *16*, 1378–1395.
5. Ban, R., Irino, Y., Fukami, K., and Tanaka, H. (2004). Human mitotic spindle-associated protein PRC1 inhibits MgcRacGAP activity toward Cdc42 during the metaphase. J. Biol. Chem. *279*, 16394–16402.
6. Bratman, S.V., and Chang, F. (2007). Stabilization of overlapping microtubules by fission yeast CLASP. Dev. Cell *13*, 812–827.
7. Gruneberg, U., Neef, R., Li, X.L., Chan, E.H.Y., Chalamalasetty, R.B., Nigg, E.A., and Barr, F.A. (2006). KIF14 and citron kinase act together to promote efficient cytokinesis. J. Cell Biol. *172*, 363–372.
8. Kurasawa, Y., Earnshaw, W.C., Mochizuki, Y., Dohmae, N., and Todokoro, K. (2004). Essential roles of KIF4 and its binding partner PRC1 in organized central spindle midzone formation. EMBO J. *23*, 3237–3248.
9. Neef, R., Gruneberg, U., Kopajtich, R., Li, X.L., Nigg, E.A., Sillje, H., and Barr, F.A. (2007). Choice of Plk1 docking partners during mitosis and cytokinesis is controlled by the activation state of Cdk1. Nat. Cell Biol. *9*, 436–444.
10. Zhu, C.J., and Jiang, W. (2005). Cell cycle-dependent translocation of PRC1 on the spindle by Kif4 is essential for midzone formation and cytokinesis. Proc. Natl. Acad. Sci. USA *102*, 343–348.
11. Kwok, B.H., Kapitein, L.C., Kim, J.H., Peterman, E.J.G., Schmidt, C.F., and Kapoor, T.M. (2006). Allosteric inhibition of kinesin-5 modulates its processive directional motility. Nat. Chem. Biol. *2*, 480–485.
12. Kapitein, L.C., Peterman, E.J.G., Kwok, B.H., Kim, J.H., Kapoor, T.M., and Schmidt, C.F. (2005). The bipolar mitotic kinesin Eg5 moves on both microtubules that it crosslinks. Nature *435*, 114–118.
13. Qian, H., Sheetz, M.P., and Elson, E.L. (1991). Single-particle tracking—analysis of diffusion and flow in 2-dimensional systems. Biophys. J. *60*, 910–921.
14. Kolin, D.L., and Wiseman, P.W. (2007). Advances in image correlation spectroscopy: Measuring number densities, aggregation states, and dynamics of fluorescently labeled macromolecules in cells. Cell Biochem. Biophys. *49*, 141–164.
15. Schnitzer, M.J. (1993). Theory of continuum random-walks and application to chemotaxis. Phys. Rev. E Stat. Phys. Plasmas Fluids Relat. Interdiscip. Topics *48*, 2553–2568.
16. Mashanov, G.I., and Molloy, J.E. (2007). Automatic detection of single fluorophores in live cells. Biophys. J. *92*, 2199–2211.